Treatment of actual radioactive wastewater containing Cs-137 using kaolinite clay minerals as eco-friendly adsorbents

Wasan A. Muslim[a], Salam K. Al-Nasri[b], Talib M. Albayati[c,]*, Hasan Sh. Majdi[d]

[a]*Iraqi Geological Survey, Ministry of Industry and Minerals, email: wasan.taee@gmail.com*
[b]*Iraqi Atomic Energy Commission (IAEC), Radiation and Nuclear Safety Directorate, Baghdad, Iraq, email: salamalnasri@gmail.com*
[c]*Department of Chemical Engineering, University of Technology, 52 Alsinaa St., P.O. Box: 35010, Baghdad, Iraq,*
email: Talib.M.Naieff@uotechnology.edu.iq
[d]*Department of Chemical Engineering and Petroleum Industries, Al-Mustaqbal University College, Babylon 51001, Iraq,*
email: hasanshker1@gmail.com

ABSTRACT

The radionuclide radiation risks brought on by nuclear weapons cannot be disregarded by the operators. To protect the public's health, radioactive cesium (Cs) polluted water must be treated with sustainable materials. In this work, batch adsorption studies were investigated to separate the radioactive isotope Cs-137 from the actual radioactive wastewater. In a batch adsorption method, the natural clay kaolinite was described and chosen as an adsorbent. After 2 h, equilibrium was attained with kaolinite having a removal efficiency of 75% for Cs-137. The adsorption kinetics of Cs-137 on the surfaces of kaolinite clay were assessed. The experimental kinetic data for kaolinite generated an outstanding match with the pseudo-first-order kinetic model. As a result, kaolinite was determined as the appropriate media to be adsorbent for Cs-137.

Keywords: Radioactive remediation; Radioactive treatment; Clay minerals; Wastewater treatment; Kaolinite; Cesium adsorption; Wastewater remediation; Radioactive isotope; Radioactive pollution

1. Introduction

Due to its substantially greater threat to both current and future generations' health, radioactive contamination has garnered more attention than chemical and biological pollution. Different kinds of radioactive material were discharged into the environment in the four well-known nuclear catastrophes, which occurred in 1957 in the UK at Windscale, 1979 in the USA at Three Mile Island, 1986 in Russia at Chernobyl, and 2011 in Japan at Fukushima [1]. Under the Al-Tuwaitha Nuclear Research Center in Iraq, which is close to the city of Baghdad, a significant amount of radioactive wastewater including Cs-137 has accumulated since 1991 [2]. Because Cs-137 has a half-life of 30 y, it is able to readily harm a number of body organs [3]. The radioactive substance Cs-137 has a significant negative impact on human health and can cause harm to several illnesses and organs, including cancer of the thyroid, liver, bladder, and kidney [4]. Different methods, such as ion exchange [5–7], chemical precipitation [8–13], membrane separation [14–16], and adsorption [17–21], are currently being studied for the treatment of water contaminated by radioactive. Adsorption has a high activity and a low operating cost, and several studies have indicated that it is an effective method for removing radioactive elements from wastewater. The removal of radioactive materials from aqueous solution has previously been examined, using artificial polymers [22], zeolite [23,24], activated carbon [25,26], and bentonite clay [27].

* Corresponding author.

The clay minerals were the best treatment medium for industrial wastewater because of their characteristics, which make them ideal adsorbents because of their availability, low cost of manufacturing, nontoxic makeup, high specific surface area, outstanding adsorption qualities, and high potential for ion exchange [28]. Kaolin is the rock term for the mineral kaolinite which is 1:1 phyllosilicate mineral. The structure of kaolinite is a tetrahedral silica sheet, alternating with an octahedral alumina sheet, joined by sharing a common layer of oxygens and hydroxyls. Large cation exchange capacities and high total uptake of cesium occur when the interlayer sites are available for adsorption [29]. Several studies inspected the mechanism of cesium adsorption by ion exchange with different potential sites on mineral surfaces and studied the effect of the structural characteristics of this clay minerals [30]. Other research examined the parameters that influence adsorption, adsorption isotherms, thermodynamics, and kinetics for many clay minerals [31].

In this work, the application of Iraqi natural clay minerals such; as kaolinite as a very cheap, environmentally friendly, most available adsorbent material in a batch adsorption system. The actual samples of radioactive wastewater containing Cs-137 have been treated using the kaolinite natural clay beyond its characterization. Furthermore, the influence of the various variables on the treatment via the adsorption process were examined. The isotherms and kinetics of adsorption were investigated as well.

2. Experimental work

2.1. Clay mineral preparation and characterization

Clays have characteristics that depend on their geological formation and mining location. Deposits of bentonite and attapulgite occur in Wadi Bashira of the Western Desert (Iraq). Kaolin clay samples were taken from the Ga'ara Depression in the Western Desert (Iraq). The kaolin clay representative samples were supplied and crushed by a jaw crusher (Retsch BB1, Germany) and then milled in a rotating cylinder ball mill to pass a 75-μ sieve opening. Chemical wet analyses to identify the chemical composition of the kaolin clay mineral was achieved in the Central Laboratories Department/Iraqi Geological Survey. X-ray diffraction mineralogical analyses were performed using the Ital Structure Model MPD 3000 (Spain, Al Razi Metallurgical Center, Tehran, Iran). Scanning electron microscopy (SEM) and energy-dispersive X-ray spectroscopy (EDX) techniques were employed to investigate the morphology of the kaolin clays with the TESCAN MIRA3 Instrument (Australia, Al Razi Metallurgical Center, Tehran, Iran). Particle-size distribution analyses were made using a Brookhaven Instruments (USA) 90Plus particle size analyzer (Nanotechnology Center, UOT, Iraq). The specific surface area (SSA) and cation exchange capacity (CEC) for the kaolin clay minerals were obtained from technical reports of the Iraqi Geological Survey (Baghdad, Iraq). The Fourier-transform infrared spectroscopy (FTIR) analyses of the kaolin clays was run with (Bomem MB-Series FTIR Spectrometer, France). According to ASTM E 1252-98(21) to specify the functional groups.

2.2. Radioactive wastewater sample preparation

The samples of the radioactive wastewater were taken from a reservoir underneath the destroyed Radiochemical Laboratories at the Al-Tuwaitha Site (Iraq). The gamma spectroscopy analysis was conducted using a closed-end, coaxial, p-type model (GEM65P4-95/ORTEC (USA, Al-Tuwaitha Site (Iraq)) high purity germanium detector (HPGe), yielding high-level waste (HLW) containing radioactive cesium (Cs-137) with a specific activity of 4.5 GBq/L [32]. As per the appropriate safety procedure (PS), the sample was diluted with distilled water to a safe limit to be handled within the laboratory. The activity was reduced to about 6,372 Bq/L, which is considered the initial activity concentration.

2.3. Batch adsorption experiments

A batch mode experiments were carried out to evaluate the use of the kaolinite Iraqi clay minerals in the adsorption of Cs-137 from the radioactive wastewater. In glass containers, a constant amount (0.1 g) of kaolinite clay was added to 30 mL of radioactive wastewater samples with a Cs-137 activity concentration of 6,372 Bq/L and a pH of 6. The sample containers were shaken on a shaking table at 200 rpm at room temperature (25°C) for different mixing times (i.e., 0.5, 1, 1.5, 2, and 3 h). At the end of mixing time, the filtration of samples was done by using a 0.45-μ Whatman™ filter. The separation of solid particles from the solution was conducted using centrifugation rather than filtration using filter paper to avoid some adsorption of contaminant in filter paper. Filtrate samples (20 mL) were put into a Marinelli Beaker to measure the radioactivity concentration of cesium after treatment, using gamma spectroscopy (HPGe detector). The Cs-137 (μg/L) concentrations in the filtrates were estimated using Eqs. (1)–(4) [33].

$$\text{Specific Activity}\,(\text{S.A.}) = \frac{\lambda \times \text{Aav} \times w}{m} \tag{1}$$

$$w = \frac{\text{S.A.} \times m}{\lambda \times \text{Aav}} \tag{2}$$

where Aav is Avogadro's number (6.02×10^{23} nuclei/mol), λ is the radioisotope decay constant (s), m is the atomic weight (g/mol), and w is the weight (g).

$$\lambda = \frac{\ln 2}{\text{half life}} = \frac{0.693}{t^{1/2}} \tag{3}$$

$$\text{Cs isotope concentration in filtrate}\,(\text{C}) = \frac{w}{v} \tag{4}$$

These clays were compared by studying the removal efficiency ($R\%$), adsorption capacity, q_e (mg/g), and adsorption coefficient, K_d (L/g), respectively, of the Cs-137 isotope at equilibrium, using Eqs. (5)–(7) [34]:

$$R\% = \frac{\text{concentration of adsorbed cesium}}{\text{initial concentration of cesium}} = \frac{C_o - C_e}{C_o} \times 100 \tag{5}$$

$$q_e = \frac{\text{amount of cesium adsorbed}}{\text{amount of adsorbent}} = \frac{(C_o - C_e) \times V}{M} \tag{6}$$

$$K_d = \frac{C_o - C_e}{C_e} \times \frac{V}{M} = \frac{q_e}{C_e} \qquad (7)$$

where C_o and C_e are the initial and equilibrium concentration of the radioactive cesium (mg/L), V is the volume of the solution (L), and M is the weight of the clay mineral materials (g).

2.4. Adsorption kinetics

The adsorption mechanism of Cs-137 on the kaolinite clay surfaces was investigated using the data resulting from the effect of contact time. The three linearized models of adsorption kinetics which applicate to evaluate the experimental result were: pseudo-first-order (Lagergren model), pseudo-second-order, and intraparticle diffusion (Weber–Morris model), which are represented by Eqs. (8)–(10), respectively [35,36].

$$\ln\left(q_e - q_t\right) = \ln q_e - k_1 t \qquad (8)$$

$$\frac{t}{q_t} = \frac{1}{k_2 q_e^2} + \frac{t}{q_e} \qquad (9)$$

$$q_t = k_p t^{1/2} + C \qquad (10)$$

where q_e and q_t are the adsorption capacity (mg/g) at equilibrium and at time t (min), respectively; k_1 and k_2 are adsorption rate constants of the pseudo-first-order (min^{-1}) and pseudo-second-order (g/mg·min), respectively; k_p is the intraparticle diffusion rate (mg/g·min$^{0.5}$) constant, and C is the diffusion intraparticle constant.

3. Results and discussion

3.1. Clay mineral characterization

The results of the chemical and mineralogical analyses for the kaolinite sample of natural clay minerals are shown in Table 1 and Fig. 1.

The theoretical chemical formula of kaolinite is 39.5% Al_2O_3, 46.5% SiO_2, and 14.0% H_2O. From Table 1 the

Table 1
Chemical analyses of kaolinite clay ore

Chemical composition	Kaolinite
SiO_2 (%)	50.22
Al_2O_3 (%)	33.52
Fe_2O_3 (%)	1.65
CaO (%)	0.32
MgO (%)	0.08
SO_3 (%)	0.07
L.O.I (%)	12.1
Na_2O (%)	0.04
K_2O (%)	0.48
Cl (%)	1.47

kaolinite sample had high content of (50.22%) of SiO_2 when compared with pure kaolin of (46.54%), the rest of the silica as quartz [37,38].

In the mineralogical analyses of kaolinite sample, the major peaks of kaolinite at diffraction angles (2θ) with (12.5° and 25°) while the minor peaks for quartz at (27°) diffraction angle as appearing in Fig. 1. Fig. 2 displays the SEM images for the kaolinite clay before and after loading with Cs-137, there was some disorder of the layered-like structure.

EDX qualitative elemental compositions analysis by identifying a material's crystal structure was achieved at a certain point referred to as (a) on the kaolinite *t* clay surfaces after adsorption, as presented in Fig. 3.

The EDX spectrum detects at that point (a) on clay surfaces for the kaolinite clay, the presence of Cs-137 by Lα and Lβ in the range of 4–5 K after adsorption of the radioactive wastewater (Fig. 3). The particle size of the kaolinite clay was investigated using a Brookhaven 90Plus particle size analyzer. This test is based on dynamic light scattering principles. The mean particle size of the kaolinite powder is presented in Fig. 4.

According to the particle size analysis, kaolinite exhibited the smallest particle size. The surface areas were calculated using the Brunauer–Emmett–Teller method. As shown in Table 2, kaolinite had the low specific surface area and cation exchange capacity.

The FTIR spectra of kaolinite before and after the cesium adsorption is shown in Fig. 5. Before the kaolinite adsorbed (KB) the following stretching vibration bands were appeared such as: Al–OH–Al, Si–O–Si, Si–OH, Al–OH, Si–O–Si/Si–O–Al, and Al–OH at 3,699/3,620; 1,032; 1,007; 912; 757 and 696 cm^{-1}, respectively. After the adsorption of kaolinite (KA) as shown in Fig. 5. (K), a new band appeared at 3,655 cm^{-1}, which means that adsorption may occur on the Al–OH–Al sites. Furthermore, the spectrum showed a slight shift on the Si–O–Si/Al–O–Si sites as it appeared at 764 cm^{-1}, while it was 757 cm^{-1} before adsorption.

3.2. Batch adsorption results

3.2.1. Activity concentration and removal %

The results of the batch adsorption experiments are shown in Fig. 6. The maximum reduction in the Cs-137
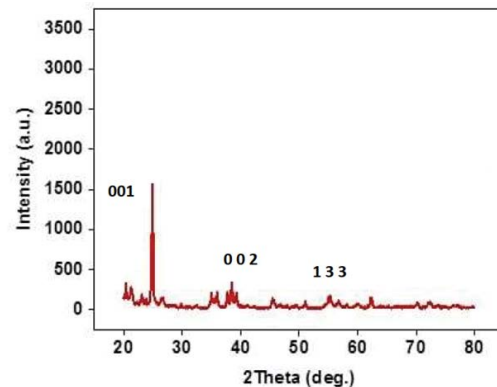

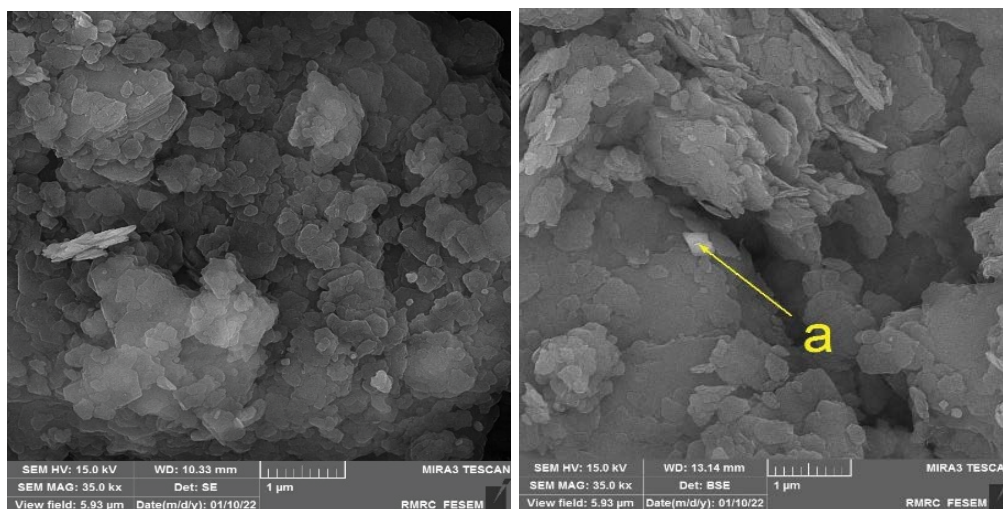Fig. 1. X-ray diffraction patterns of kaolinite clay ores.

Fig. 2. Scanning electron microscopy images for the kaolinite clays. a: certain point on the three clay surfaces analyzed after adsorption.
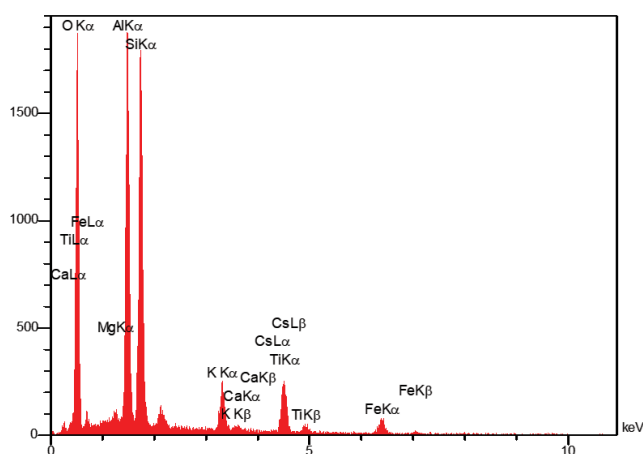

Fig. 3. Energy-dispersive X-ray spectroscopy analysis of the kaolinite clays after adsorption.

Fig. 4. Particle size analyses for the kaolinite clay.

Table 2
Mean particle size with a specific surface area for the kaolinite

Sample	Kaolinite
Mean particle diameter (nm)	61.3
St. deviation	1.07
Density (g/cm³)	2.6
CEC (meq./100 g)	3.5
Specific surface area (SSA) m²/g	37.6

activity concentration was achieved at 304 Bq/L during the 2 h that it took for the uptake of cesium to reach equilibrium for kaolinite. The $R\%$ of the adsorption results were determined from Eq. (5). However, at an equilibrium time of 2 h, the removal efficiencies reached 75% for kaolinite, as illustrated in Fig. 6. The removal efficiency of kaolinite decreased after 3 h of adsorption time. This convergence in the removal efficiencies could be the result of the rapprochement in the chemical and mineralogical compositions of the kaolinite clays as displayed in Table 1 [18].

3.2.2. Mechanisms of Cs sorption

In kaolin clay the active sites locate only in type (I) the planar (basal) surface and type (II) the edges of the interlayers which show low cation exchange capacity compared with that of type (III). Since the kaolinite structure does not expand, kaolinite does not tightly adsorb Cs in its struct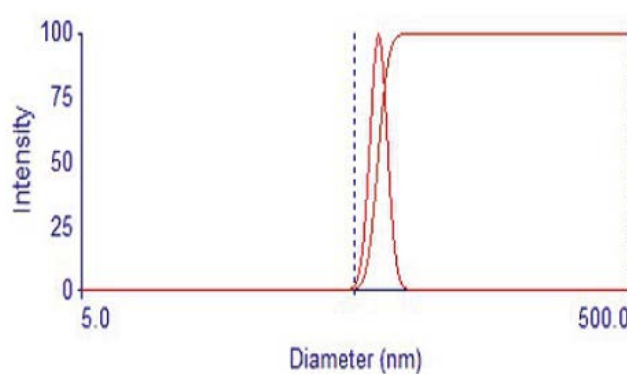ure, it is interstratified with vermiculite and micaceous layers [39]. In case of kaolinite the ion exchange capability is due to broken bonds at the edges of the clay planes and to hydroxyl groups on the basal lamellar. These results indicate that Cs is adsorbed not only at the "frayed edge" site, but also at other sites where Cs is reversibly adsorbed as reported by the study of Erten et al. [40] and Shahwan et al. [41]. Comans and Hockley [42] and Comans et al. [43] have proposed a model with two different mechanisms of Cs sorption. One of these mechanisms is instantaneous and reversible on a timescale of a few days and less. The other is irreversible, occurs at longer times, and is caused by Cs

migration into the interlayers. Slow Cs migration into inter-layers was also proposed by Evans et al. [44]. These agreed with the decrees of cesium adsorption (desorption) by kaolinite after 2 h in the results as clarified in Fig. 6b because some of the cesium site reversible on the basal planes of kaolinite.

3.2.3. Adsorption capacity and distribution coefficient

The adsorption capacity (q_e) and adsorption distribution coefficient (K_d) for the kaolinite clay minerals at different contact times were calculated from Eqs. (6) and (7), respectively. The adsorption capacity (q_e) and adsorption distribution coefficient (K_d) for the kaolinite clay minerals can be seen in Fig. 7a and b, respectively. These results clarified that the prime adsorption distribution coefficient (K_d) and adsorption capacity (q_e) obtained for kaolinite after 2 h of contact time were caused by using a very low Cs-137 initial activity concentration, owing to the fact that the sorption increased sharply at the low sorbate initial concentration [45,46].
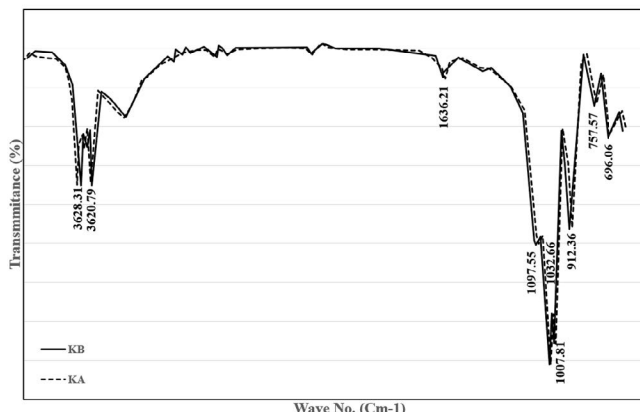
Fig. 5. Fourier-transform infrared spectra of kaolinite before adsorption (KB) and after adsorption (KA).
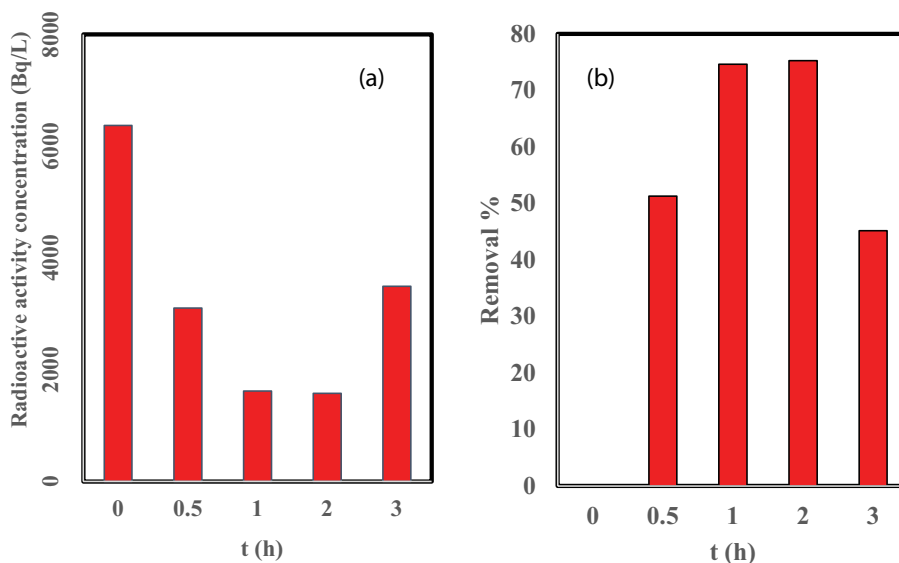
3.3. Adsorption kinetics

The results of the submitted kinetic models—pseudo-first-order [Eq. (8)], pseudo-second-order [Eq. (9)], and intraparticle diffusion [Eq. (10)] are displayed in Fig. 8a–c, respectively, for the kaolinite clay mineral. The adsorption mechanisms of Cs-137 for the kaolinite clay mineral better fit the pseudo-first-order kinetic model with a high regression coefficient, (0.9169) compared with the pseudo-second-order model (0.9018), respectively.

The predicted adsorption capacity (q_e) by the pseudo-first-order model for kaolinite approached the experimental adsorption capacity (q_e), as illustrated in Table 3.

The intraparticle diffusion adsorption kinetic model is based on the assumption that the rate-controlling step may involve valence forces through ion exchange, substitution, or complexation (Wei et al. [47] and Al-Rahmani et al. [48]). Since the plot of q_t vs. $t^{(0.5)}$ in the intraparticle model, as shown in Fig. 8c, did not pass the through the origin, intraparticle diffusion did not completely affect the adsorption process. Also, the correlation coefficient (R^2) of the diffusion model was lower than the pseudo-first and second-order correlation coefficient for kaolinite, as shown in Table 3. The convenience of the pseudo-first-order model with the experimental result means that the adsorption is controlled by ionic exchange, in which electrostatic interactions played a significant part [47,48].

3.4. Comparative study

A comparison between the results of this study and previous studies is illustrated in Table 4. This table offers important details regarding how effectively kaolinite adsorbent may increase Cs-137 capacity for adsorption from other adsorbent materials. Kaolinite has an excellent adsorption efficiencies of Cs-137 were achieved by kaolinite (75%) for a 2-h equilibrium time without functionalization or treatment of its surface. One may conclude that adding a functional group to the surface of kaolinite will increase its adsorption
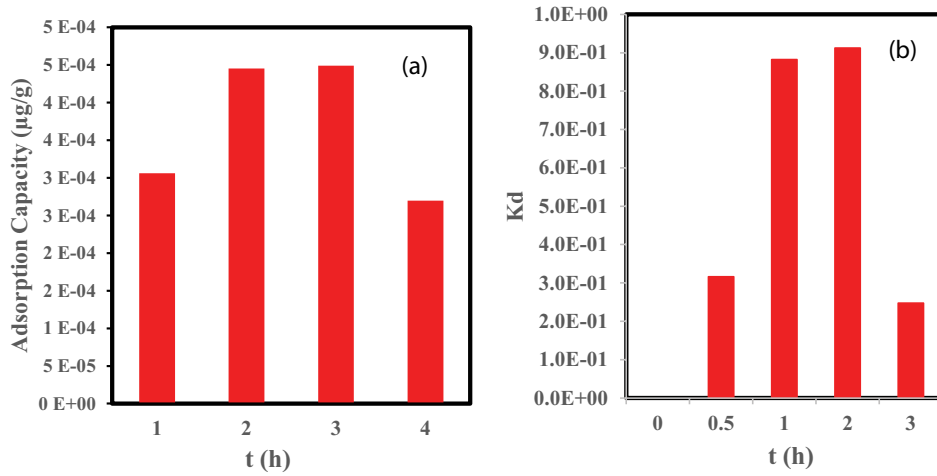
Fig. 6. Effect of contact time on (a) activity concentration and (b) removal % of Cs-137 from radioactive wastewater for kaolinite.

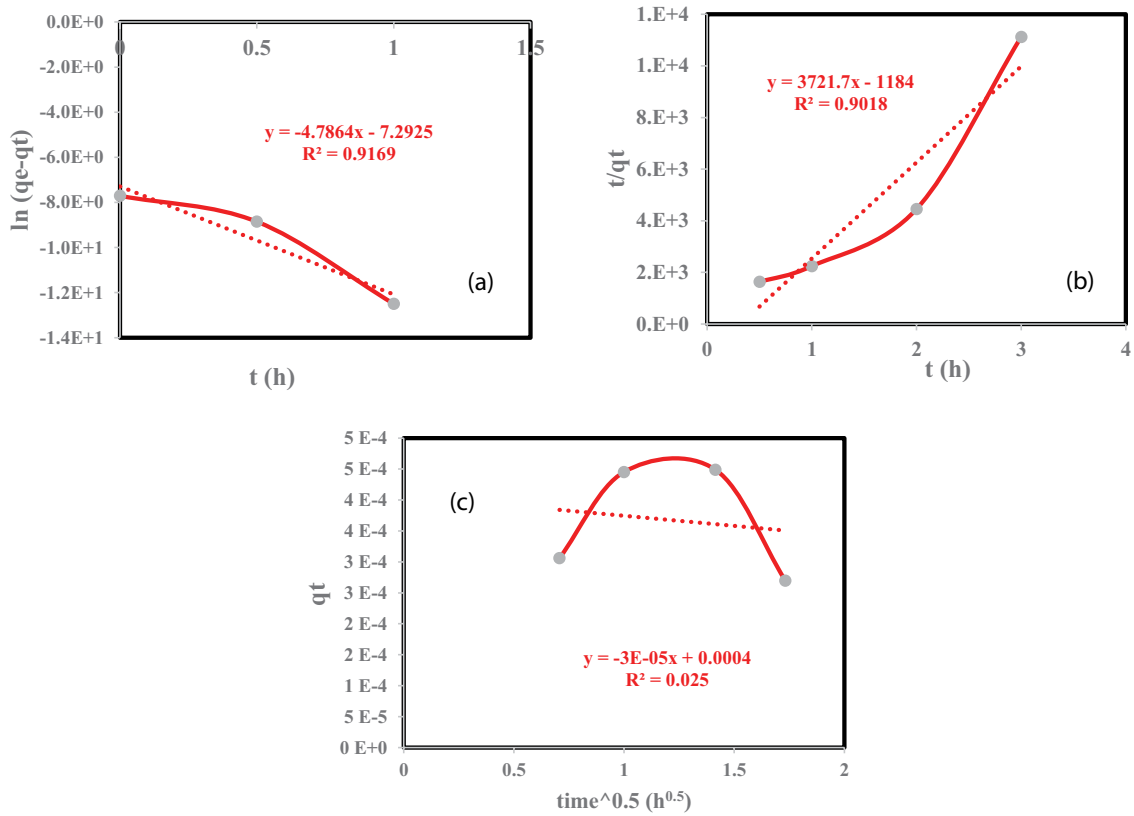Fig. 7. (a) Adsorption capacity (q_e) and (b) adsorption distribution coefficient (K_d) for kaolinite.

Fig. 8. Adsorption kinetic models for kaolinite (a) pseudo-first-order adsorption kinetic model, (b) pseudo-second-order adsorption kinetic model and (c) intraparticle diffusion adsorption kinetic model.

Table 3
Kinetic models parameters for the adsorption of kaolinite

	Experimental	Pseudo-first-order model		Pseudo-second-order model		Intraparticle diffusion model	
	q_e (mg/g)	q_e (mg/g)	R^2	q_e (mg/g)	R^2	C (mg/g)	R^2
Kaolinite	0.45E-6	0.26E-6	0.917	0.26E-6	0.9018	0.4	0.025

Table 4
Adsorption capacities of Cs-137 by various adsorbents

Adsorbents	Adsorption capacity Q_{max} (mg/g)	Removal efficiency %	Equilibrium time	References
Nanocomposites	280.82	NA	24 h	Jang and Lee [49]
Nanoparticles with PEG	274.70	64.8	1 h	Qian et al. [50]
Microparticles	16.30	97.0	10 min	Wang et al. [51]
Cobalt hexacyanoferrate	92.12	NA	4 h	Yousefi et al. [52]
Charcoal modified	133	99	220 min	Nazmul Hasan et al. [53]
Kaolinite	NA	75	2 h	This study

capacity. This result suggest that kaolinite is strong, stable, and efficient sorbents for Cs-137 removal compared with other various kinds of modified adsorbents. Moreover, kaolinite is easily applied as adsorbents with a natural, low cost, eco-friendly, and simple batch sorption process compared with synthesized adsorbents, such as zeolites, composites, and bio-sorbents for Cs-137 radioactive decontamination.

4. Conclusion

Bentonite and attapulgite had the smallest particle size and the highest specific surface area, they have better cation exchangeability and, effective functional sites than kaolinite. Excellent adsorption efficiencies of the Cs-137 isotope were achieved by bentonite (98%) and attapulgite (97%) for a 2-h equilibrium time. During 2 h of contact time, kaolinite only exhibited an acceptable adsorption efficiency (75%) of the Cs-137 isotope, but this efficiency decreases after 2-h of contact time which could be a desorption of the Cs-137 isotope to solution. Therefore, kaolinite clay neither efficient nor stable in the Cs-137 adsorption. The high values of adsorption achieved in this study resulted from the use of low-radioactivity concentrations of Cs-137 (~6.372 KBq/L). The kinetics of Cs-137 adsorption on the three clay surfaces were evaluated. The pseudo-second-order kinetic model produced an excellent fit with the experimental kinetic data for bentonite and attapulgite. According to the results, the local raw bentonite and attapulgite were the most suitable clays (which should be selected rather than the other phyllosilicate clays, such kaolinite) to manage the decontamination process of the Cs-137 isotope from wastewater. Therefore, the three chosen adsorbents proved to be promising materials for the removal of the radioactive isotope Cs-137 because they are inexpensive, available, and effective adsorbent materials.

Declarations

Ethics approval and consent to participate

Not applicable.

Competing interests

The authors declare that they have no competing interests.

Consent for publication

Not applicable.

Availability of data and material

All relevant data and material are presented in the main paper.

References

[1] Y. Liu, P. Gu, L. Jia, G. Zhang, An investigation into the use of cuprous chloride for the removal of radioactive iodide from aqueous solutions, J. Hazard. Mater., 302 (2016) 82–89.

[2] M.A. Cherif, A. Martin-Garin, F. Gérard, O. Bildstein, A robust and parsimonious model for caesium sorption on clay minerals and natural clay materials, Appl. Geochem., 87 (2017) 22–37.

[3] S.R.H. Vanderheyden, R. Van Ammel, K. Sobiech-Matura, K. Vanreppelen, S. Schreurs, W. Schroeyers, J. Yperman, R. Carleer, Adsorption of cesium on different types of activated carbon, J. Radioanal. Nucl. Chem., 310 (2016) 301–310.

[4] I.T. Al-Alawy, O.A. Mzher, Radiological characterization of the irt-5000(14-Tammuz) research nuclear reactor at Al-Tuwaitha nuclear center in Iraq, Environ. Earth Sci., 78 (2019) 229, doi: 10.1007/s12665-019-8122-6.

[5] S. Higaki, M. Hirota, Decontamination efficiencies of pot-type water purifiers for ^{131}I, ^{134}Cs and ^{137}Cs in rainwater contaminated during Fukushima Daiichi nuclear disaster, PLoS One, 7 (2012) e37184, doi: 10.1371/journal.pone.0037184.

[6] C. Decamp, S. Happel, Utilization of a mixed-bed column for the removal of iodine from radioactive process waste solutions, J. Radioanal. Nucl. Chem., 298 (2013) 763–767.

[7] S. Sarri, P. Misaelides, F. Noli, L. Papadopoulou, D. Zamboulis, Removal of iodide from aqueous solutions by polyethylenimine-epichlorohydrin resins, J. Radioanal. Nucl. Chem., 298 (2013) 399–403.

[8] N.M. Jabbar, S.M. Alardhi, A.K. Mohammed, I.K. Salih, T.M. Albayati, Challenges in the implementation of bioremediation processes in petroleum-contaminated soils: a review, Environ. Nanotechnol. Monit. Manage., 18 (2022) 100694, doi: 10.1016/j.enmm.2022.100694.

[9] N.S. Ali, K.R. Kalash, A.N. Ahmed, T.M. Albayati, Performance of a solar photocatalysis reactor as pretreatment for wastewater via UV, UV/TiO$_2$, and UV/H$_2$O$_2$ to control membrane fouling, Sci. Rep., 12 (2022) 16782, doi: 10.1038/s41598-022-20984-0.

[10] G. Lefèvre, A. Walcarius, J.-J. Ehrhardt, J. Bessière, Sorption of iodide on cuprite (Cu_2O), Langmuir, 16 (2000) 4519–4527.

[11] A.N. Kamenskaya, N.B. Mikheev, S.A. Kulyukhin, I.A. Rumer, V.L. Novichenko, Metal-containing zeolites as sorbents for localization of radioiodine and CsI aerosols from vapor-air and aqueous phases, Radiochemistry, 43 (2001) 575–579.

[12] G. Lefèvre, J. Bessière, J.-J. Ehrhardt, A. Walcarius, Immobilization of iodide on copper(I) sulfide minerals, J. Environ. Radioact., 70 (2003) 73–83.

[13] S.D. Balsley, P.V. Brady, J.L. Krumhansl, H.L. Anderson, Iodide retention by metal sulfide surfaces: cinnabar and chalcocite, Environ. Sci. Technol., 30 (1996) 3025–3027.

[14] D. Rana, T. Matsuura, M.A. Kassim, A.F. Ismail, Radioactive decontamination of water by membrane processes — a review, Desalination, 321 (2013) 77–92.

[15] G. Zakrzewska-Trznadel, Advances in membrane technologies for the treatment of liquid radioactive waste, Desalination, 321 (2013) 119–130.

[16] S.M. Alardhi, J.M. Alrubaye, T.M. Albayati, Removal of methyl green dye from simulated wastewater using hollow fiber ultrafiltration membrane, IOP Conf. Ser.: Mater. Sci. Eng., 928 (2020) 052020, doi: 10.1088/1757-899X/928/5/052020.

[17] S. Choung, W. Um, M. Kim, M.-G. Kim, Uptake mechanism for iodine species to black carbon, Environ. Sci. Technol., 47 (2013) 10349–10355.

[18] J.S. Hoskins, T. Karanfil, S.M. Serkiz, Removal and sequestration of iodide using silver-impregnated activated carbon, Environ. Sci. Technol., 36 (2002) 784–789.

[19] H.J. Al-Jaaf, N.S. Ali, S.M. Alardhi, T.M. Albayati, Implementing eggplant peels as an efficient bio-adsorbent for treatment of oily domestic wastewater, Desal. Water Treat., 245 (2022) 226–237.

[20] N.S. Ali, N.M. Jabbar, S.M. Alardhi, H.Sh. Majdi, T.M. Albayati, Adsorption of methyl violet dye onto a prepared bio-adsorbent from date seeds: isotherm, kinetics, and thermodynamic studies, Heliyon, 8 (2022) e10276, doi: 10.1016/j.heliyon.2022.e10276.

[21] M. Ikari, Y. Matsui, Y. Suzuki, T. Matsushita, N. Shirasaki, Removal of iodide from water by chlorination and subsequent adsorption on powdered activated carbon, Water Res., 68 (2015) 227–237.

[22] A. Iwanade, N. Kasai, H. Hoshina, Y. Ueki, S. Saiki, N. Seko, Hybrid grafted ion exchanger for decontamination of radioactive cesium in Fukushima Prefecture and other contaminated areas, J. Radioanal. Nucl. Chem., 293 (2012) 703–709.

[23] P. Rajec, F. Macášek, M. Féder, P. Misaelides, E. Šamajová, Sorption of caesium and strontium on clinoptilolite-and mordenite-containing sedimentary rocks, J. Radioanal. Nucl. Chem., 229 (1998) 49–55.

[24] K.C. Song, H.D. Kim, H.K. Lee, H.S. Park, K.J. Lee, Adsorption characteristics of radiotoxic cesium and iodine from low-level liquid wastes, J. Radioanal. Nucl. Chem., 223 (1997) 199–205.

[25] S.T. Kadhum, G.Y. Alkindi, T.M. Albayati, Determination of chemical oxygen demand for phenolic compounds from oil refinery wastewater implementing different methods, Desal. Water Treat., 231 (2021) 44–53.

[26] T. Kubota, S. Fukutani, T. Ohta, Y. Mahara, Removal of radioactive cesium, strontium, and iodine from natural waters using bentonite, zeolite, and activated carbon, J. Radioanal. Nucl. Chem., 296 (2013) 981–984.

[27] W.A. Muslim, S.K. Al-Nasri, T.M. Albayati, Evaluation of bentonite, attapulgite, and kaolinite as eco-friendly adsorbents in the treatment of real radioactive wastewater containing Cs-137, Prog. Nucl. Energy, 162 (2023) 104730, doi: 10.1016/j.pnucene.2023.104730.

[28] G.D. Yuan, B.K.G. Theng, G.J. Churchman, W.P. Gates, Chapter 5.1 – Clays and Clay Minerals for Pollution Control, F. Bergaya, G. Lagaly, Eds., Developments in Clay Science, Elsevier, Vol. 5, 2013, pp. 587–644, ISSN 1572-4352, ISBN 9780080993645. Available at: https://doi.org/10.1016/B978-0-08-098259-5.00021-4

[29] T. Ohnuki, N. Kozai, Adsorption behavior of radioactive cesium by non-mica minerals, J. Nucl. Sci. Technol., 50 (2013) 369–375.

[30] Y. Zabulonov, V. Kadoshnikov, H. Zadvernyuk, T. Melnychenko, V. Molochko, Effect of the surface hydration of clay minerals on the adsorption of cesium and strontium from dilute solutions, Adsorption, 27 (2021) 41–48.

[31] W.A. Muslim, T.M. Albayati, S.K. Al-Nasri, Decontamination of actual radioactive wastewater containing ^{137}Cs using bentonite as a natural adsorbent: equilibrium, kinetics, and thermodynamic studies, Sci. Rep., 12 (2022) 13837, doi: 10.1038/s41598-022-18202-y.

[32] Z.H. Ibrahim, A.F. Mkhaiber, S.K. Al-Nasri, Estimation and reduction of the total activity for the liquid waste pool in radiochemistry laboratories in Al-Tuwaitha site, Baghdad J. Eng. Appl. Sci., 13 (2018) 3386–3391.

[33] G.F. Knoll, A.V. Wegst, Radiation detection and measurement, Med. Phys.: Int. J. Med. Phys. Res. Pract., 7 (1980) 397–398.

[34] N.S. Abbood, N.S. Ali, E.H. Khader, H. Sh. Majdi, T.M. Albayati, N.M. Cata Saady, Photocatalytic degradation of cefotaxime pharmaceutical compounds onto a modified nanocatalyst, Res. Chem. Intermed., 49 (2023) 43–56.

[35] A.T. Khadim, T.M. Albayati, N.M. Cata Saady, Removal of sulfur compounds from real diesel fuel employing the encapsulated mesoporous material adsorbent Co/MCM-41 in a fixed-bed column, Microporous Mesoporous Mater., 341 (2022) 112020, doi: 10.1016/j.micromeso.2022.112020.

[36] N.S. Ali, H.N. Harharah, I.K. Salih, N.M. Cata Saady, S. Zendehboudi, T.M. Albayati, Applying MCM-48 mesoporous material, equilibrium, isotherm, and mechanism for the effective adsorption of 4-nitroaniline from wastewater, Sci. Rep., 13 (2023) 9837, doi: 10.1038/s41598-023-37090-4.

[37] A.W.A. Al-Ajeel, S.N. Abdullah, A.M. Kh. Mustafa, Beneficiation of attapulgite – montmorillonite claystone by dispersion sedimentation, Iraqi Bull. Geol. Min., 4 (2008) 117–124.

[38] M.I. Abdou, A.M. Al-sabagh, M.M. Dardir, 2013, Evaluation of Egyptian bentonite and nano-bentonite as drilling mud, Egypt. J. Pet., 22 (2013) 53–59.

[39] R.L. Frost, Hydroxyl deformation in kaolins, Clays Clay Miner., 46 (1998) 280–289.

[40] H.N. Erten, S. Aksoyoglu, S. Hatipoglu, H. Göktürk, Sorption of cesium and strontium on montmorillonite and kaolinite, Radiochim. Acta, 44–45 (1998) 147–152.

[41] T. Shahwan, H.N. Erten, L. Black, G.C. Allen, TO-SIMS study of Cs^+ sorption on natural 647 kaolinite, Sci. Total Environ., 226 (1999) 255–260.

[42] R.N.J. Comans, D.E. Hockley, Kinetics of cesium sorption on illite, Geochim. Cosmochim. Acta, 56 (1992) 1157–1164.

[43] R.N.J. Comans, M. Haller, P. De Preter, Sorption of cesium on illite: non-equilibrium behaviour and reversibility, Geochim. Cosmochim. Acta, 55 (1991) 433–440.

[44] D.W. Evans, J.J. Alberts, R.A. Clark III, Reversible ion-exchange fixation of cesium-137 leading to mobilization from reservoir sediments, Geochim. Cosmochim. Acta, 47 (1983) 1041–1049.

[45] T. Missana, A. Benedicto, M. García-Gutiérrez, U. Alonso, Modeling cesium retention onto Na-, K- and Ca-smectite: effects of ionic strength, exchange and competing cations on the determination of selectivity coefficients, Geochim. Cosmochim. Acta, 128 (2014) 266–277.

[46] L. Baborová, D. Vopálka, R. Červinka, Sorption of Sr and Cs onto Czech natural bentonite: experiments and modelling, J. Radioanal. Nucl. Chem., 318 (2018) 2257–2262.

[47] X. Wei, Y. Sun, D. Pan, Z. Niu, Z. Xu, Y. Jiang, W. Wu, Z. Li, L. Zhang, Q. Fan, Adsorption properties of Na-palygorskite for Cs sequestration: effect of pH, ionic strength, humic acid and temperature, Appl. Clay Sci., 183 (2019) 105363, doi: 10.1016/j.clay.2019.105363.

[48] A.A. Al-Rahmani, S.K. Al-Attafi, S.K. Al-Nasri, Z.W. Jasim, Hierarchical structures incorporating carbon and zeolite to remove radioactive contamination, Iraqi J. Sci., 61 (2020) 1944–1951.

[49] J. Jang, D.S. Lee, Magnetic prussian blue nanocomposites for effective cesium removal from aqueous solution, Ind. Eng. Chem. Res., 55 (2016) 3852–3860.

[50] J. Qian, J.Y. Xu, L.J. Kuang, D.B. Hua, Cesium removal from human blood by poly(ethylene glycol)-decorated prussian blue magnetic nanoparticles, ChemPlusChem, 82 (2017) 888–895.

[51] P.F. Wang, J.L. Zheng, X.L. Ma, X. Du, F.F. Gao, X.G. Hao, B. Tang, A. Abudula, G. Guan, Electroactive magnetic microparticles for the selective elimination of cesium ions in the wastewater, Environ. Res., 185 (2020) 109474, doi: 10.1016/j.envres.2020.109474.

[52] T. Yousefi, M. Torab-Mostaedi, M.A. Moosavian, H.G. Mobtaker, Potential application of a nanocomposite:HCNFe@polymer for effective removal of Cs(I) from nuclear waste, Prog. Nucl. Energy, 85 (2015) 631–639.

[53] Md. Nazmul Hasan, M.A. Shenashen, Md. Munjur Hasan, H. Znad, Md. Rabiul Awual, Assessing of cesium removal from wastewater using functionalized wood cellulosic adsorbent, Chemosphere, 270 (2021) 128668, doi: 10.1016/j.chemosphere.2020.128668.